# DYNAMIC RESPONSE MONITORING OF FLIGHT CONTROL WITH INCREMENTAL NONLINEAR DYNAMIC INVERSION

Hannes Hofsäß<sup>1</sup> & Florian Holzapfel<sup>2</sup>

<sup>1</sup>Technical University of Munich, Institute of Flight System Dynamics, Garching, D-85748, Germany

#### **Abstract**

Runtime monitoring is a key element in safety critical flight control applications, where fault tolerance is often achieved by automatic failure detection and subsequent reconfiguration. Model-based runtime monitoring uses knowledge of the system dynamics in order to detect incompliant behavior. In this paper, a novel model structure for model-based monitoring of closed-loop systems is proposed, that is inspired by an extended incremental nonlinear dynamic inversion control approach. It ensures that the dynamics of the monitoring models reflect the relative degree of the plant including its actuator dynamics. The model structure thereby allows decoupling of residual signals from the control input as the lag in the response to control inputs is correctly incorporated in the model. Monitoring of allowable intervals for dynamic responses is enabled by integration of the model structure with a method for model-based monitoring of uncertain systems. Considering its application in the domain of flight control, the resulting monitor requires no physical modelling of the aircraft and allows to account for the effect of additional lag in the closed-loop's response due to the dynamics of the actuation system. Thus, failure detection capability with respect to allowable system responses derived from high-level requirements is improved. The approaches effectiveness is demonstrated in a simulative use case for runtime response monitoring of requirements from ADS-33E-PRF with a nonlinear model of a piloted vertical take-off and landing aircraft in hover flight. Results of optimization-based worst-case analysis are presented in order to assess the monitor's proneness to generate false alarms. The improved capability to detect failures in the presence of uncertainty is finally validated through numerical simulations.

**Keywords:** Model-Based Monitoring; Runtime Monitoring; Incremental Flight Control

## 1. Introduction

Safety assurance is a central aspect in the development of digital aerial control systems. For safety critical flight control software, high validation and verification (V&V) efforts are demanded in order to provide confidence that errors have been removed during design time. Hence, full V&V of novel control approaches with inherent increased software complexity may be challenging and safety assurance during runtime is considered as an alternative [1]. In order to ensure safety by means of physical state constraints, fallback control system designs that base on set invariance theory have been proposed [2], [3]. While formal guarantees with respect to the state constraints can be given, hazards that may result from incompliant aircraft response to inputs at the pilot's control inceptors, with the aircraft remaining within the constrained state space, are not covered. In [4], the potentially catastrophic event of Loss-of-control has been characterized not only by violation of normal flight envelopes, but also as "a motion that is not predictably altered by pilot control inputs". Pilot induced oscillations that result from such degraded aircraft response to inceptor inputs furthermore have been identified a major cause for Loss-of-control. Hence, ensuring compliance to state constraints only is not sufficient for safety if hazards, that result from incompliant aircraft response to pilot inputs, shall be mitigated. In order to address this gap, model-based failure detection of the aircraft response has been proposed [5]. Based on high-level aircraft response requirements, the expected response

<sup>&</sup>lt;sup>2</sup>Technical University of Munich, Institute of Flight System Dynamics, Garching, D-85748, Germany

of an aircraft's short-period motion is given by runtime execution of a linear system model and incompliant response can be identified through appropriate selection of the failure detection threshold. False alarms that may result from higher order dynamics of the plant, when only low-order dynamics are considered in the monitoring model, are not regarded. In [6], a model-based monitoring method is proposed that captures allowable parametric intervals by incrementally simulating the dynamics of the uncertainty space only at it's corner points. If monotonicity of the uncertain dynamics is given with respect to the uncertain parameters, upper and lower bounds for measurements can be obtained from the incremental simulations. The approach is extended in [7] in order to additionally propagate stochastic uncertainties through linear dynamics, thereby providing stochastically motivated boundaries for the measurements that are used for compliance monitoring. The author proposes to derive the monitoring models by numerical linearization, which implies a dependency on the accuracy of the utilized model. Furthermore, effects of actuator dynamics are not covered.

In this paper, a novel model structure for model-based runtime monitoring of closed-loop system responses is proposed. The structure is inspired by the derivation of an extended incremental nonlinear dynamic inversion (INDI) control approach that was proposed in [8]. The order of the monitoring dynamics is derived from the relative degree of the plant including actuator dynamics. Hence, the physically driven lag in the response of the system's outputs with respect to control inputs is correctly accounted for, which improves decoupling of residuals from the control input. Furthermore, model dependency with respect to physical plant-parameters is low, as no physical modelling is required. In the scope of monitoring of an aircraft's response to pilot inputs, its application allows to address uncertainty in the aircraft's response on acceleration level, which is highly affected by actuator dynamics. Thus, monitoring performance with respect to false alarms and missed detections is improved.

The paper further contributes through validation of the proposed structure in a simulative use case with a high-fidelity model of a piloted vertical take-off and landing (VTOL) aircraft in hover flight. A demonstration of model-based monitoring for runtime verification of dynamic response requirements with a high-fidelity nonlinear aircraft model advances the maturity and applicability of the approach and has, to the best of the author's knowledge, not been reported yet.

The remainder of the paper is structured as follows: In section 2. the extended INDI control law as proposed in [8], and the herein integrated method for model-based monitoring of uncertain systems from [6], are briefly introduced. Next, the structure of the monitoring-models is derived, and a description of the logics included for failure detection is provided. Finally, we analyze the effects of higher order actuator dynamics onto the residuals of the detection logics. In section 3. , the monitoring approach is demonstrated in a use case with a high fidelity flight-dynamical model of a VTOL aircraft that is controlled by the control law for simplified vehicle operations developed in [9]. A monitoring design is derived, that bases on dynamic response requirements from ADS-33E-PRF [10]. Its robustness towards false positive alarms due to arbitrary sequences of input signals at the pilot inceptor is validated through optimization-based worst-case analysis. Finally the improvement of the monitor's capability for failure detection is demonstrated in numerical simulations and section 4. provides a conclusion and an outlook on future work.

## 2. Derivation of the Monitor

In this section, the model-based runtime monitor is derived. Firstly, the extended INDI control law is introduced. Secondly, the method for online monitoring applied in this paper is described. Thirdly, the proposed model structure is presented and finally robustness towards structural modelling uncertainties is analyzed.

#### 2.1 The extended INDI control law

INDI is a sensor-based control approach that utilizes feedback of the state derivative in order to reduce model dependency to an estimation of the control effectiveness. Though actuator dynamics are usually neglected, their effect is considered in the INDI control law design in [11]. In order to account for actuators with differing dynamics, an extension has been proposed in [8]. Furthermore, the controller designed for simplified vehicle operation of VTOL aircraft proposed in [9] implements the extended approach. In this paper, a model structure for model-based runtime monitoring is derived that aims to account for the lag in the closed-loop's response to control inputs. The extended INDI

#### Dynamic Response Monitoring of Flight Control with Incremental Nonlinear Dynamic Inversion

approach inherently addresses this aspect by consideration of the plant's relative degree and the additional lag resulting from actuator dynamics. Hence, the model structure is derived from the closed-loop response provided by the extended INDI control approach. Therefore, the derivation of the extended INDI control approach is briefly introduced next. The system dynamics are given as

$$\dot{x}(t) = f(x(t), u(t))$$

$$y(t) = h(x(t)),$$
(1)

with the state  $x \in \mathbb{R}^{n_x}$ , control input  $u \in \mathbb{R}^{n_u}$ , and output  $y \in \mathbb{R}^{n_y}$ . Furthermore the functions  $f : (\mathbb{R}^{n_x} \times \mathbb{R}^{n_u}) \to \mathbb{R}^{n_x}$  and  $h : \mathbb{R}^{n_x} \to \mathbb{R}^{n_y}$  are k+2 times differentiable mappings. The dependency on the time is omitted in the following in order to simplify the notation. The output can be differentiated k times until the control input u explicitly appears. The resulting transformed system is given by

$$y^{(k)} = F(x, u), \tag{2}$$

with a subsequent chain of k integrators applied on  $y^{(k)}$  in order to obtain the higher channel system outputs. Now, first order actuator dynamics are considered and one further derivative allows to include the actuator states into the system dynamics. It yields

$$y^{(k+1)} = F_x \dot{x} + F_u \dot{u},\tag{3}$$

with the partial derivatives  $F_x = \frac{\partial F(u,x)}{\partial x}$  and  $F_u = \frac{\partial F(u,x)}{\partial u}$ . In the following, the state dependent term is neglected [8] [12] and first order actuator dynamics are given as

$$\dot{u} = K_a(u_c - u),\tag{4}$$

with the diagonal matrix  $K_a$  that contains inverted time constants of the actuator dynamics along its diagonal elements. The incremental control law can now be obtained by

$$u_c = (F_u K_a)^+ v + u, \tag{5}$$

with the Moore-Penrose inverse  $(F_uK_a)^+$  rendering a right inverse of  $(F_uK_a)$  assuming  $F_u$  has full row rank. Finally, the pseudo control v is chosen as

$$v = k_v (y_c^{(k)} - y^{(k)}) \tag{6}$$

in [8]. Hence, a first-order response of the actuation system to the commanded output  $y_c^{(k)}$  is obtained. Note that the dynamics of Eq.(6) will, in the case of aircraft control, specify the desired dynamics for forces and moments produced by the actuation system. In the following, we will refer to these dynamics as the inner-loop dynamics. The derivation above only holds in case that no model uncertainty is considered for the actuation bandwidth and the control effectiveness, which will not reflect reality. In order to demonstrate the effect of uncertainty, we consider a one dimensional motion and replace the uncertain parameters in the control law with their estimates  $\hat{F}_u\hat{K}_a$ . We get

$$u_c = \left(\hat{F}_u \hat{K}_a\right)^+ v + u. \tag{7}$$

Inserting the law in the dynamics of Eq. (3) and neglecting the state dependent term gives

$$y^{(k+1)} = F_u K_a \left(\hat{F}_u \hat{K}_a\right)^+ k_v (y_c^{(k)} - y^{(k)}).$$
(8)

Here, the term  $F_uK_a(\hat{F}_u\hat{K}_a)^+$  denotes a scalar and thus the model uncertainty affects the bandwidth of the inner-loop. Hence, it can be concluded that model uncertainty affects the bandwidth of the inner-loop and propagates upwards through the chain of integrators.

# 2.2 Model-Based Monitoring with Imprecise Dynamics

Having introduced the control law, the design of the monitor is addressed next. For that purpose, the model-based method for system response monitoring initially proposed in [6] and further extended in [7] is used in this paper and will briefly be introduced.

For systems with a known structure but uncertain parameters, the uncertain parameter intervals can be defined in an  $n \times 2$  dimensional vector p with

$$p = [(p_{1,lo}, p_{1,up}) (p_{2,lo}, p_{2,up}) \dots (p_{n,lo}, p_{n,up})]^T$$
(9)

with lo and up giving the lower and upper bounds of the respective interval. As proposed in [6], the trajectories of the system that are affected by the uncertainty can be bounded by evaluation of the system's dynamics only at the  $2^n$  corner points of the uncertainty space given in vector p. The resulting set of systems can be describe by

$$X(t) = \{x_i(t) : \dot{x}_i(t) = f(x_i(t), u(t), p_i)\}\$$

$$Y(t) = \{y_i(t) : y_i(t) = g(x_i(t), p_i)\},$$
(10)

with  $i \in [1,...,2^n]$ . Additionally, in order for the states in the equation above to bound the trajectories, the states at the corner points must change monotonously with respect to the uncertain parameters p. Monotonicity can be decided by considering the states sensitivity with respect to p which is given by

$$\frac{dW(t,x,p)}{dt} = A(t,x,p)W(t,x,p) + V(t,x,p), \tag{11}$$

with

$$a(t,i,j) = \frac{\partial \dot{x}(t,x,p)}{\partial x_{j}},$$

$$v(t,i,j) = \frac{\partial \dot{x}(t,x,p)}{\partial p_{j}},$$

$$w(t,i,j) = \frac{dx(t,p)}{dp_{j}},$$

$$W(0,x_{0},p) = 0$$
(12)

and hence, monotonicity is given if all entries w(t,i,j) have the same sign [6]. For linear dynamics, stochastic uncertainties that result from measurement inaccuracies and process noise can be covered by additionally propagating the uncertainties through the set of dynamics described by Eq. (10) as proposed in [7]. Furthermore, the check for monotonicity is only fulfilled for limited simulation intervals of the system's corner dynamics. Thus, it is proposed in [7] to reset of the simulated states on the measurements frequently. The resulting short simulation intervals decrease the methods sensitivity to detect incompliant system response. However, it has been demonstrated in [7], that monotonicity is given most of the time for simulation intervals that are required for effective failure detection.

## 2.3 Monitoring of Uncertain Aircraft Response

In [7], the method introduced above is applied for model-based monitoring of the vertical distance of two large fixed-wing aircraft. The models are derived by linearization of the longitudinal dynamics and the effect of actuator dynamics on the response of aircraft-level moments is neglected. Thus, the effect of actuator dynamics on the inner-loop is reflected in the model structure for online monitoring in this paper. Furthermore, parametric uncertainty in the inner-loop's dynamics is accounted for in the model, while the effect of structural uncertainty is analyzed qualitatively. For derivation of the model structure, the transformed system dynamics from Eqs. (6) and (3) is applied. Hence, the set of allowable dynamics yields

$$Y_{\mathsf{m}}^{(0)} = \{y_{\mathsf{m},i}^{(0)}\}$$

$$\vdots$$

$$Y_{\mathsf{m}}^{(k)} = \{y_{\mathsf{m},i}^{(k)}\}$$

$$Y_{\mathsf{m}}^{(k+1)} = \{y_{\mathsf{m},i}^{(k+1)} : y_{\mathsf{m},i}^{(k+1)} = k_{\mathsf{v},j}(y_{\mathsf{m},\mathsf{c},i}^{(k)} - y_{\mathsf{m},i}^{(k)})\},$$

$$(13)$$

with  $i \in [1...2^n]$ ,  $j \in \{\text{up,lo}\}$  and  $y_{\text{m,c},i}^{(k)}$  can be designed arbitrarily in order to provide the required response of the higher level states. For that purpose n uncertain parameters may be used in addition to  $k_{v,j}$ . The higher level states  $y_{\text{m,i}}^{(k)}...y_{\text{m,i}}^{(0)}$  can be obtained by successive integration. Additional mapping functions can be included to reflect kinematic couplings between the response variables. An example is given in the later presented use case. Note that no physical modelling of the aircraft is required, as the model structure reflects a desired aircraft response. Actuator dynamics are inherently accounted for by the uncertain outputs  $Y_{\text{m}}^{(k+1)}$ , that could be interpreted as a set of allowable aircraft-level jerks. Next, the failure detection logics of the monitor are defined. As described in the section above, the states need to be reset frequently in order to achieve monotonicity for most of the time. Here, we choose the initial values to be the measurements, which allows to include stochastic uncertainty in the bounds for the allowable trajectories as proposed in [7]. In order to finally detect incompliant system response, we introduce the residual logic similar to [6] that yields

$$r_{k,\text{lo}} = y^{(k)} - y_{\text{lo}}^{(k)},$$
  
 $r_{k,\text{up}} = y^{(k)} - y_{\text{up}}^{(k)},$  (14)

with  $y_{\text{lo}}^{(k)} = \min\{y_{\text{m},i}^{(k)}\}$  and  $y_{\text{up}}^{(k)} = \max\{y_{\text{m},i}^{(k)}\}$ . Further residual signals can be defined accordingly for the remaining measurements of  $y^{(k-1)}...y^0$ . Finally, incompliant system response is detected if

$$(r_{k,\mathsf{lo}} < 0 \lor r_{k,\mathsf{up}} > 0) \land (\mathsf{sgn}(w_{i,j,\mathsf{min}}) = \mathsf{sgn}(w_{i,j,\mathsf{max}}))$$

$$\tag{15}$$

holds. The described derivation renders the first novelty of this paper. Based on the transformed system dynamics derived in the extended INDI control approach, a generic structure of the set of allowable closed-loop dynamics is provided, which is suitable for derivation of the monitoring models. It ensures that the dynamics of monitoring models account for the system's relative degree including its actuator dynamics. As the relative degree provides a measure of the minimum lag of the system output with respect to the control input [13], its consideration in the monitoring-model improves decoupling of the residuals from the closed-loop input. Furthermore, no modelling of physical system-coefficients is required. In the scope of monitoring of an aircraft's response to pilot inputs, its application allows to account for the additional lag that results from actuator dynamics in the monitoring model. Thereby, performance with respect to false alarms and failure detection capability is improved. A demonstration of the proposed modelling structure's effectiveness is provided in a use case in the next section.

In the following, a qualitative analysis of the monitor's robustness with respect to structural model errors is provided. For that purpose we assume that the system is controlled by a control law as presented in section 2.1, which is not required for the application of the model structure in general. Having introduced the residual signals, the effect of higher order actuator dynamics in the closed-loop system can be observed in the linear frequency response of the residuals to desired inputs  $y_c^{(k)}$ . The transformed system dynamics from Eq. (8) essentially consists of a first order response to  $y_c^{(k)}$ , and a successive chain of integrators. Thus, assuming constant control effectiveness  $F_u$  and second order actuator dynamics, a second order response of  $y_c^{(k)}$  is produced, that is modelled by including another derivative in the dynamics of Eq.(8). It yields

$$y^{(k+2)} = k_{\mathbf{a}}(k_{\mathbf{v}}(y_{\mathbf{c}}^{(k)} - y^{(k)}) - y^{(k+1)}).$$
(16)

For derivation of the equation above  $k_a$  can be referred to as an inner-loop parameter of the actuator dynamics. As residuals are defined on each level of integration as given in Eq. (14), the structural mismatch propagates to the upper level residuals through the chain of integrators. The effect can be obtained from Fig 1 for the dynamics introduced so far and k=2. Here, the transfer functions from input  $y_c^{(2)}$  to  $r_2$ ,  $r_1$  and  $r_0$  are considered, with the residuals  $r_k = y^{(k)} - y_m^{(k)}$ ,  $y_m^{(k)}$  as in Eq. (13) if no parametric uncertainties are present. Furthermore  $y_c^{(k)} = y_{m,c}^{(k)}$  is assumed, and thus only the structural mismatch between the first order actuator dynamics assumed in the monitor and the respective second order dynamics of the system excites a response of the residual signals. As each

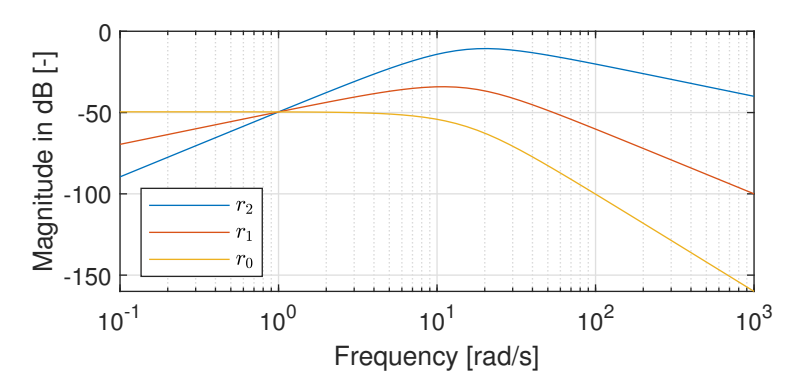


Figure 1 – Frequency response of residuals  $r_k$  to command signals  $y_c^{(k)}$ , assuming  $y_c^{(k)} = y_{m,c}^{(k)}$ , no parametric uncertainty and the closed-loop system to include second order actuator dynamics. The model used for monitoring assumes first order inner-loop dynamics from Eq. (13) which excites the residuals on the respective integration levels.

integrator reduces the residual magnification at high frequency inputs but increases them at the low frequencies, it can be concluded that magnification of unconsidered higher order actuator dynamics that may trigger false monitoring alarms can be reduced by choosing only the residuals with small peak gains for runtime monitoring.

# 3. Monitoring of the Dynamic Response of a VTOL Aircraft in Hover Flight

In this section, we apply the introduced model structure in a simulative use case for monitoring of a VTOL aircraft's lateral dynamics in hover flight. First, we describe the system consisting of a nonlinear VTOL aircraft model, a control law and the model-based monitor. Next, an analysis of the monitor's failure detection performance is provided that focuses on the effect of uncertain inner-loop dynamics. Therefore, we evaluate the monitor's robustness towards false alarms in the presence of uncertain inner-loop dynamics. Finally, we analyze it's capability of detecting failed responses with respect to requirements from ADS-33E-PRF [10]. The use case renders the second contribution of this paper. A demonstration of model-based dynamic response monitoring for compliance to handling qualities requirements with a nonlinear high-fidelity aircraft model has, to the best of the author's knowledge, not been reported yet. Thereby, this section contributes by advancing the maturity and applicability of online dynamic response monitoring for flight control.

## 3.1 System Description

The aircraft model used in this section implements the rigid body equations of motion of a VTOL aircraft and includes lookup tables that reflect aircraft and propeller aerodynamics. Control effectors are arranged in a *lift+cruise* configuration and thus lift is provided by multiple propeller engines that produce thrust along the aircraft's vertical axis in hover flight. Additionally, the model features higher order models for electro-mechanical actuators that include modelling of electrical current limitations. Furthermore the model includes a digital flight control law that implements the extended INDI-type control law from Eqs. (5), (6) and realizes a translational rate command response type as specified in ADS-33E-PRF, a military standard that includes performance specifications and Handling Qualities Requirements [10]. The control law has been designed in [9] in order to implement a concept for simplified vehicle operations. The aircraft model has been used for simulative validation in [9] and [14], and furthermore worst-case analysis of the setup has been performed in [15]. In the following, the monitoring design is derived and the uncertain parameter space is presented.

In hover flight, the pilot is able to command yaw rate  $\psi$  and kinematic velocities in the C-frame, which relates to the north-east-down frame by a rotation around the aircraft's heading [9]. In this use case, we only consider tracking of the lateral velocity  $V_{C,y}$ . As the aircraft has a *lift+cruise* configuration, lateral motion is created through excitation of the roll angle  $\phi$  in order to provide the lateral acceleration  $\dot{V}_{C,y}$ . It can be modelled by

$$\dot{V}_{C,v} = -\sin(\phi_{\mathsf{m}}) f_{B,z} \tag{17}$$

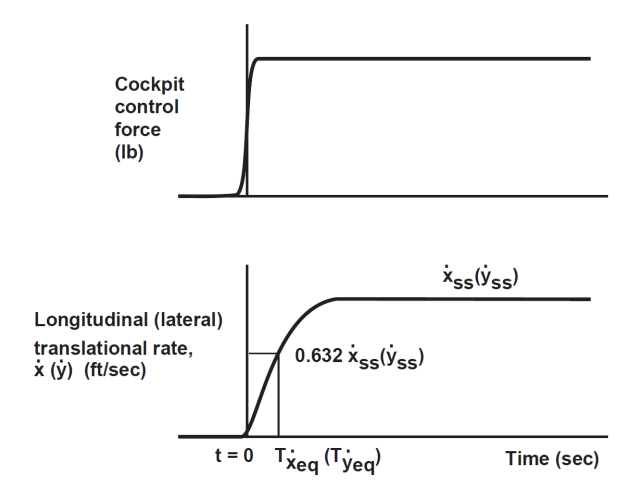


Figure 2 – Definition of equivalent rise time as given in [10].

for the herein considered one dimensional motion. Thus, an aircraft-level angular acceleration  $\ddot{\phi}$ needs to be provided by control of the lift propellers rotational speeds, resulting in a system relative degree of k=3. Applying the structure for the monitoring dynamics given in Eq. (13), we can express the aircraft's lateral dynamics with

$$\ddot{\phi}_{m} = k_{V} \left[ k_{\dot{\phi}} \left( a \sin \left( \frac{\omega_{0}^{2} (V_{C,y,\text{des}} - V_{C,y,m})}{-f_{B,z}} \right) - 2\omega_{0} \zeta \phi_{m} - \dot{\phi}_{m} \right) - \ddot{\phi}_{m} \right], \tag{18}$$

where  $V_{C,y,\text{des}}$  is the desired lateral velocity. Furthermore, the modelled roll angle and its derivatives  $\phi_m$ ,  $\dot{\phi}_m$ ,  $\ddot{\phi}_m$  are obtained by respective integration of  $\ddot{\phi}_m$  and the modelled lateral Velocity  $V_{C,y,m}$  is given by integration of it's derivative  $\dot{V}_{C,y,m}$ , which follows Eq.(17). The body-fixed vertical specific force  $f_{B,z}$ can be obtained from the measurements. Finally,  $\omega_0$ ,  $\zeta$ ,  $k_{\phi}$  and  $k_{\nu}$  denote the design parameters that shape the dynamic response of the lateral velocity  $V_{C,y,m}$ . Next, the requirement considered for specification of dynamic responses to inputs  $V_{C,v,des}$  is introduced. In ADS-33E-PRF [10] allowable dynamic responses to pilot inceptor inputs are specified for translational rate response type aircraft by means of an equivalent rise time parameter that is given in Fig. 2. The parameter for equivalent rise time  $T_{\dot{y},eq}$  shall remain between 2.5 and 5 seconds. The smaller limit intends to bound the abruptness of attitude changes for aircraft configurations that use attitude for generation of horizontal acceleration [16] like it is done in the configuration considered here. As  $k_{\nu} \in [k_{\nu,lo} \ k_{\nu,up}]$  reflects the uncertain inner-loop dynamics, we further shape the allowable responses with  $\omega_0 \in [\omega_{0,\mathsf{up}} \ \omega_{0,\mathsf{lo}}]$  and hence the uncertain parameter space is given by

$$p = [(\omega_{0,\text{lo}} \ \omega_{0,\text{up}}) \ (k_{\nu,\text{lo}} \ k_{\nu,\text{up}})]^T.$$
(19)

Furthermore, we choose  $\zeta$  and  $k_\phi$  to be constant here for simplicity. Hence, we can tune the overall allowable response quickness of  $V_{C,y}$  with the parameter space of  $\omega_0$  and additionally account for the uncertain response of the inner-loop by defining the parameter space of  $k_{\nu}$ .

In the following, we apply the introduced monitoring model to the simulation environment that includes the nonlinear model of the VTOL aircraft and the control law. Though in [6] and [7] it is suggested to use each measurement update to re-initialize the states of the monitoring-models, the simulation intervals need to be at least larger than the sample time of the monitoring software, if it shall be considered for real world application in a digital flight control system. Hence, a simulation interval of 0.1 seconds is chosen here. As higher order dynamics of the actuators are not reflected in the monitoring model, the residuals for failure detection are only considered for the lateral velocity and its derivative, such that the structural discrepancy has negligible effect on the residuals. Therefore, the definition of the residuals yields

$$r_{0,\mathsf{up}} = V_{C,y} - V_{C,y,up} + \Delta_{V_C}, r_{1,\mathsf{up}} = \dot{V}_{C,y} - \dot{V}_{C,y,up} + \Delta_{\dot{V}_C}, 7$$
 (20)

with the residuals for the lower limits being defined accordingly. The constant margins  $\Delta$  are introduced for additional robustness towards false alarms that may result from nonlinearities of the system that are not reflected in the models for monitoring. The values chosen here increase robustness towards false positive failure detections on the one hand, but also decrease the sensitivity of the failure detection on the other hand. Therefore, the procedure for their tuning is the following:

- Initially, no constant margins are included and the worst-case residuals are obtained for the closed-loop controlled aircraft with the desired inner-loop's bandwidth of the controller  $k_{v,c}$  set to the lower boundary of the allowable uncertainty. It is chosen in a way that the requirements on equivalent rise remain fulfilled for the aircraft model controlled by the controller. A set of margins is then obtained for the case that the uncertainty is implemented in the monitoring model's parameter  $k_v$ , as well as for the case that does not consider the uncertainty.
- Next, the failure detection capability of both monitors with integrated margins is compared in a step response scenario. Here, we set the controller's inner-loop bandwidth parameter  $k_{v,c}$  to be smaller then the minimum value of the uncertainty interval considered for  $k_v$  in order to simulate a degraded aircraft response that violates the requirements.

## 3.2 False Positive Analysis

Here, we analyze the monitors robustness towards false alarms, that may be triggered by the input sequence for the desired lateral velocity  $V_{C,y,\rm des}$  by means of an optimization based worst-case analysis. The utilized optimization framework has been applied for worst-case analysis in the scope of aircraft flight control systems in [15], [17] and [18]. It bases on a Double Deep Q-Network agent that is trained over multiple simulation runs, also called episodes, in order to maximize a predefined scalar reward that can be obtained with a predefined set of actions, also called the action space. During each simulation run, the agent draws multiple actions from the action space and hence each run provides an action sequence with an associated reward. The training process itself thereby renders the optimization process and the action sequence that could obtain the maximum reward is considered the worst-case. More details on the method can be found in [15]. A simulation environment has been set up that includes the model of the VTOL aircraft, the control law and the monitor described above. Here, the actions provided for the optimization agent constitute a limited set of normalized pilot inceptor displacements  $\delta_{\rm S}$  that result in the desired velocities  $V_{C,y,{\rm des}}$  after an input scaling module which is not further specified here. The normalized action space has been chosen to be

$$\mathscr{A} = \{ \delta_s : \delta_s \in \{-1, -0.5, -0.3, -0.15, 0, 0.15, 0.3, 0.5, 1\} \}. \tag{21}$$

and the parameters for the Double Deep Q-Network agent have been adopted from [17]. The worst-case trajectories provided by the optimization agent for the two cases of uncertain and uncertainty-free inner-loop dynamics in the monitoring models are is given in Fig. 3. Here, the reward function was chosen to maximize the residual  $r_{1,up}$  and hence only the lateral accelerations are considered for optimization. The lower plots in the figure contain the maximum residuals achieved during the simulation run if monotonicity of the is given. Clearly, it can be obtained, that a comparatively large residual can be achieved if the monitor assumes no uncertainty in the inner-loop, whereas it remains small if the uncertainty is accounted for. In the following these values are included as the margins  $\Delta_{\hat{V}_C}$  for the two monitoring cases, and the resulting capability for failure detection is analyzed.

## 3.3 Missed Detection Analysis

Next, the effects of uncertainty in the inner-loop's bandwidth onto the high-level aircraft response to pilot inputs and the respective capability for failure detection is analyzed. The system's step responses for ideal and off-nominal inner-loop bandwidth are shown in Fig. 4. The trajectories of  $V_{C,y,\text{des}}$  result from a step input at the pilot inceptor. Fastest and slowest responses of the set of uncertain dynamics from Eqs. (17), (18) and (19) are given by  $\bar{V}_{C,y,\text{up}}$  and  $\bar{V}_{C,y,\text{lo}}$  and are designed to fulfill the requirements on equivalent rise time from ADS-33E-PRF [10] as in Fig. 2. In order to simulate off-nominal closed-loop response due to inner-loop failures, the inner-loop bandwidth parameter  $k_{v,\text{c}}$  of the controller can be adapted. Thus,  $k_{v,\text{c}}$  has been reduced here in the control law from the ideal

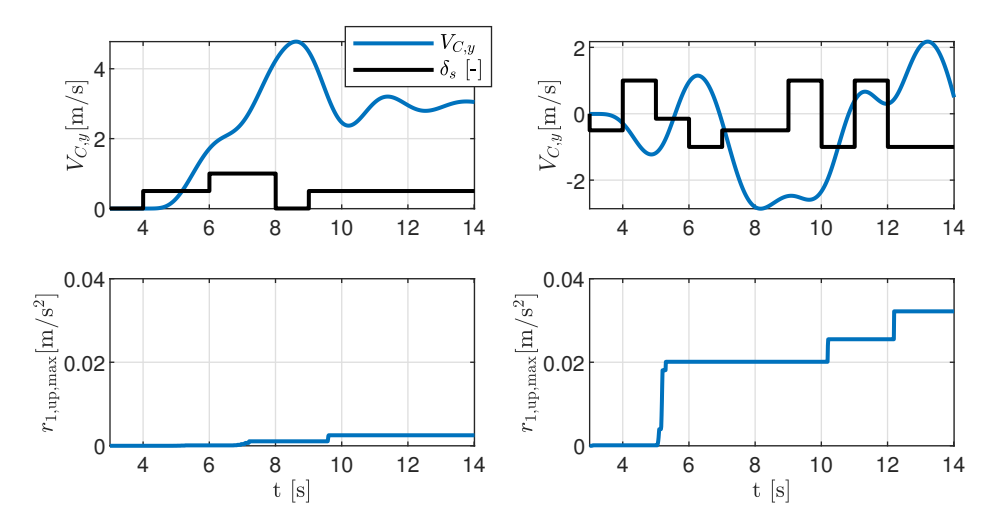


Figure 3 – Worst-Case residuals  $r_{1,up}$  (bottom) with according trajectories for normalized inceptor displacement  $\delta_s$  and lateral velocity  $V_{C,y}$ . The inner-loop bandwidth of the controlled aircraft model is set to  $k_{v,c} = k_{v,lo}$ . Left:  $\Delta_{\dot{V}} = 0$ , with uncertain inner-loop bandwidth in the monitoring models, Right:  $\Delta_{\dot{V}} = 0$  with nominal inner-loop bandwidth in the monitoring models.

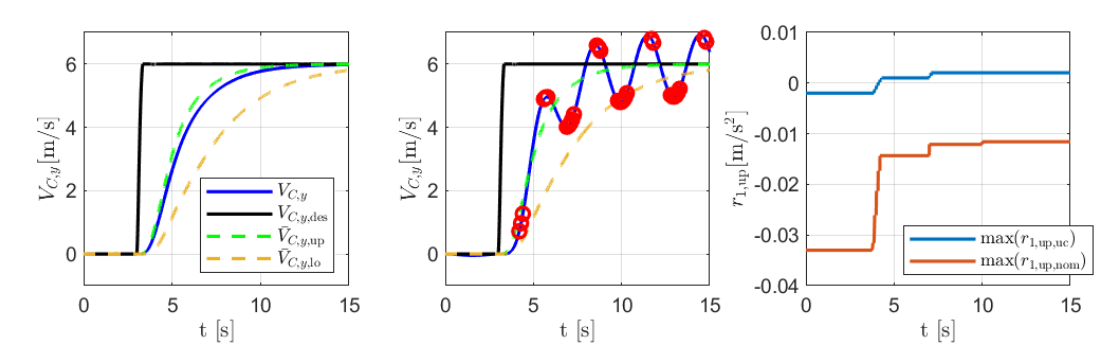


Figure 4 – Step responses of the closed-loop controlled aircraft model. Left: nominal response. Center: degraded response with inner-loop bandwidth of the controller  $k_{v,c} < k_{v,lo}$ . Instances of failure detections of the monitor that includes uncertain inner-loop dynamics are denoted with red markers. Right: Maximum obtained residuals of the monitor that includes inner-loop uncertainties (blue) and the monitor that assumes exact, nominal inner loop dynamics (red).

value of 15 to 1.5. The step responses can be obtained from Fig. 4. Though the aircraft response remains stable in the centered plot, the slow inner-loop dynamics cause a violation of the upper velocity limit  $\bar{V}_{C,y,up}$  after 4.7 seconds, which suggests an overly abrupt attitude response, and furthermore causes high oscillations in the velocity response. The red markers in the centered plot illustrate the time instances when a failure is detected by the monitor that includes inner-loop uncertainty and the margins gathered from the section above. It can be observed that the failed response is rapidly detected, which is also indicated by the trajectory of the corresponding maximum residual signal (blue) in the right plot. As before,  $\max(r_{1,up})$  gives the maximum residual obtained during the simulation run at a given time, if monotonicity is given. Due to the high constant margins required to compensate the inner-loop's uncertainty, the trajectory of the maximum residual in red remains smaller then zero. Thus, the failed response remains undetected by the monitor that implements a constant and ideal inner-loop bandwidth. It results that the  $\Delta_{\hat{V}C,y}$  required to avoid false positive alarms hides the failed aircraft response as  $\max(r_{1,up,nom})(t) < 0$  and hence the scenario renders a missed detection. Finally, it can be concluded that the failed response remains undetectable if the uncertain inner-loop dynamics are not implemented in the monitor and robustness towards false alarms is required.

#### 4. Conclusion

In this paper, a novel model structure for model-based monitoring is proposed, that bases on the transformed dynamical system considered in the derivation of an extended INDI-type control law. Thus, it accounts for the system's relative degree including actuator dynamics in order to decouple the residual signals from the control input. As dynamic response requirements are often expressed through intervals for allowable high-level response measures, the monitoring model fulfils the set of allowable responses by integrating a method for imprecise modelling. Robustness towards structural uncertainty that results from high order actuator dynamics is addressed qualitatively. Hence, the derived monitoring approach allows to tightly monitor the correctness of the input-response with respect to high level requirements while achieving robustness towards false positive failure detections.

The effectiveness of the monitoring is demonstrated in a simulation-based use case for monitoring of the closed-loop response of a VTOL aircraft in hover flight. A monitor is designed for verification of the aircraft's input-response with respect to requirements from ADS-33E-PRF. The analysis points out the importance of modelling the closed-loop's inner-loop dynamics, which is mainly driven by the dynamics of the actuation system, in the monitor. The use case adds to the state of the art, as it demonstrates the applicability of model-based runtime monitoring of dynamic response requirements in a high-fidelity simulation, which has not been reported yet. Future work includes application of the model structure for monitoring in the presence of stochastic disturbances like measurement noise or exogenous disturbance inputs.

## 5. Contact Author Email Address

Mailto: hannes.hofsaess@tum.de

## 6. Copyright Statement

The authors confirm that they, and/or their company or organization, hold copyright on all of the original material included in this paper. The authors also confirm that they have obtained permission, from the copyright holder of any third party material included in this paper, to publish it as part of their paper. The authors confirm that they give permission, or have obtained permission from the copyright holder of this paper, for the publication and distribution of this paper as part of the ICAS proceedings or as individual off-prints from the proceedings.

## **References**

- [1] John Schierman, David Ward, Brian Dutoi, Anthony Aiello, John Berryman, Michael DeVore, Walter Storm, and Jason Wadley. Run-time verification and validation for safety-critical flight control systems. In *AIAA Guidance, Navigation and Control Conference and Exhibit*, 2012.
- [2] Aaron D. Ames, Xiangru Xu, Jessy W. Grizzle, and Paulo Tabuada. Control barrier function based quadratic programs for safety critical systems. *IEEE Transactions on Automatic Control*, 62(8):3861–3876, 2017.
- [3] Thomas Gurriet, Andrew Singletary, Jacob Reher, Laurent Ciarletta, Eric Feron, and Aaron Ames. Towards a framework for realizable safety critical control through active set invariance. In 2018 ACM/IEEE 9th International Conference on Cyber-Physical Systems (ICCPS), pages 98–106, 2018.
- [4] James Wilborn and John Foster. Defining commercial transport loss-of-control: A quantitative approach. In AIAA Atmospheric Flight Mechanics Conference and Exhibit, 2004.
- [5] Markus Kaminski. *A Rapid Robust Fault Detection Algorithm for Flight Control Reconfiguration*. PhD thesis, Technische Universität München, 2019.
- [6] B. Rinner and U. Weiss. Online monitoring by dynamically refining imprecise models. *IEEE Transactions on Systems, Man, and Cybernetics, Part B (Cybernetics)*, 34(4):1811–1822, 2004.
- [7] David Löbl. *A Total Capability Approach for the Development of Safety-Critical Functions*. PhD thesis, Technische Universität München, 2018.
- [8] Stefan A. Raab, Jiannan Zhang, Pranav Bhardwaj, and Florian Holzapfel. Consideration of control effector dynamics and saturations in an extended indi approach. 2019.
- [9] Jorg Nicolai Angelov. *Model-Based Systems Engineering of Flight Control for VTOL Transition Aircraft.* PhD thesis, Technische Universität München, 2023.
- [10] Aeronautical design standard, performance specification, handling qualities requirements for military rotorcraft. Standard, United States Army Aviation And Missile Command, 2000.

## Dynamic Response Monitoring of Flight Control with Incremental Nonlinear Dynamic Inversion

- [11] Ewoud J. J. Smeur, Qiping Chu, and Guido C. H. E. de Croon. Adaptive incremental nonlinear dynamic inversion for attitude control of micro air vehicles. *Journal of Guidance, Control, and Dynamics*, 39(3):450–461, 2016.
- [12] Rasmus Steffensen, Agnes Steinert, and Ewoud J. J. Smeur. Nonlinear dynamic inversion with actuator dynamics: An incremental control perspective. *Journal of Guidance, Control, and Dynamics*, 46(4):709–717, 2023.
- [13] Florian Holzapfel. *Nonlinear Adaptive Control of an Unmanned Aerial Vehicle*. PhD thesis, Technische Universität München, 2004.
- [14] Valentin Adamov Marvakov. *Automating the Transition of Lift-to-Cruise eVTOL Aircraft*. PhD thesis, Technische Universität München, 2023.
- [15] David Braun, Michael M. Marb, Jorg Angelov, Maximilian Wechner, and Florian Holzapfel. Worst-case analysis of complex nonlinear flight control designs using deep q-learning. *Journal of Guidance, Control, and Dynamics*, 46(7):1365–1377, 2023.
- [16] Background information and user's guide (biug) for handling qualities requirements for military rotorcraft. Report, Commander, U.S. Army Research, Development, and Engineering Command, 2015.
- [17] Hannes Hofsäß, David Braun, and Florian Holzapfel. Counter optimization-based validation of flight control system monitoring. In *AIAA AVIATION 2023 Forum*, 2023.
- [18] David Braun, Rasmus Steffensen, Agnes Steinert, and Florian Holzapfel. Counter optimization-based testing of flight envelope protections in a fly-by-wire control law using deep q-learning. In CEAS EuroGNC 2022 "Conference on Guidance, Navigation and Control", 2022.